

Cyano-Bridged *d*–*f* Ensembles of the Dysprosium Tetrapyridine Complexes with the Hexacyanoferrate Anion

S. P. Petrosyants^a, * A. B. Ilyukhin^a, N. N. Efimov^a, and V. M. Novotortsev^a

^aKurnakov Institute of General and Inorganic Chemistry, Russian Academy of Sciences, Moscow, 119991 Russia

*e-mail: petros@igic.ras.ru

Received March 5, 2018

Abstract—The reactions of $\text{DyX}_3 \cdot 6\text{H}_2\text{O}$ ($\text{X} = \text{NCS, Cl}$) with 2,2':6',2"-terpyridine (Terpy) and $\text{K}_3\text{Fe}(\text{CN})_6$ in aqueous-alcohol solutions afford cyano-bridged ensembles $[\text{Dy}(\text{Terpy})(\text{H}_2\text{O})_3\text{Fe}(\text{CN})_6] \cdot n\text{H}_2\text{O}$, $[\text{Dy}_2(\text{Terpy})_2(\text{H}_2\text{O})_3(\text{CO}_3)(\text{NCS})\text{Fe}(\text{CN})_6] \cdot 4\text{H}_2\text{O}$, and $[\text{Dy}_2(\text{Terpy})_2(\text{H}_2\text{O})_4(\text{CO}_3)(\text{NCS})\text{Fe}(\text{CN})_6] \cdot 11.4\text{H}_2\text{O}$. The compounds obtained are identified by the data of elemental analysis, IR spectroscopy, X-ray diffraction analysis, and X-ray structure analysis (CIF files CCDC nos. 1827138–1827140). The study of the magnetic properties of complex $[\text{Dy}(\text{Terpy})(\text{H}_2\text{O})_3\text{Fe}(\text{CN})_6] \cdot n\text{H}_2\text{O}$ shows the low-spin state of Fe^{3+} . The dynamic magnetic behavior of this complex exhibits a slow magnetic relaxation.

Keywords: dysprosium, terpyridine, $\text{K}_3\text{Fe}(\text{CN})_6$, X-ray structure analysis, magnetic properties

DOI: 10.1134/S1070328418110064

INTRODUCTION

Octahedral cyanide anions $[\text{M}(\text{CN})_6]^{3-}$ ($\text{M} = \text{Cr, Mn, Co, Fe, and others}$) are potential N-donor ligands. The binding of $[\text{M}(\text{CN})_6]^{3-}$ with M_A^{n+} cations through the nitrogen atom of the cyanide group results in the formation of compounds with structural variability and diversity of chemical and physical properties [1–4]. As a rule, the interaction with the cyanide anion occurs in the presence of a blocking ligand that occupies certain positions in the coordination sphere of the M_A^{n+} cation thus preventing the uncontrolled formation of the cyanide bridges $\text{M}_A^{n+}\text{—NC—M}$. Three-charge cations of rare-earth elements exhibit an enhanced tendency to the coordination of the N-donor ligands along with a special oxophilicity [5]. Therefore, N-donor, mono- and polydentate, or macrocyclic ligands are often used for blocking in the case of rare-earth elements. When 2,2-bipyridine (Bipy) is chosen as a blocking ligand, the reactions of $\text{Ln}(\text{NO}_3)_3$ ($\text{Ln} = \text{Sm, Gd, Yb}$ [6] and $\text{Eu, Tb, Dy, Ho, Er, Tm, Lu}$ [7]) with $\text{M}(\text{CN})_6^{3-}$ ($\text{M} = \text{Co, Fe}$) afford complexes with the cyano-bridged chain structure. The $\text{Ln}(\text{III})\text{—Fe}(\text{III})$ interaction for the DyFe and TbFe samples was established to be antiferromagnetic, and no appreciable magnetic interactions were revealed in the cases of EuFe, HoFe, ErFe, and TmFe [6, 7]. The cyano-bridged chain compounds Sm—NC—Fe and Sm—NC—Cr in which Sm(III) ferromagnetically interacts with Fe(III) or Cr(III) through the cyanide bridges were isolated with the bidentate ligand 3,4,7,8-

tetramethyl-1,10-phenanthroline (Me_4Phen) [8]. A series of cyanide-bridged 1D compounds $\{[\text{Ln}(\text{Tptz})(\text{H}_2\text{O})_4\text{Fe}(\text{CN})_6] \cdot n\text{H}_2\text{O}\}_\infty$ for $\text{Ln} = \text{Pr, Nd, Sm, Eu, Gd, and Tb}$ was synthesized using tridentate planar 2,4,6-tris(2-pyridyl)-1,3,5-triazine (Tptz) as a blocking ligand, and among them only Sm—NC—Fe exhibits the ferromagnetic interaction with Fe(III) [8].

In this work, the tridentate ligand 2,2':6',2"-terpyridine (Terpy) was chosen as a blocking ligand. Two chelating rings in this ligand makes the Ln—Terpy binding stronger compared to similar complexes with Bipy and Phen. The reactions of the dysprosium salts with $\text{K}_3\text{Fe}(\text{CN})_6$ in the presence of Terpy gave the cyano-bridged chain compounds $[\text{Dy}(\text{Terpy})(\text{H}_2\text{O})_3\text{Fe}(\text{CN})_6] \cdot n\text{H}_2\text{O}$ (I), $[\text{Dy}_2(\text{Terpy})_2(\text{H}_2\text{O})_3(\text{CO}_3)(\text{NCS})\text{Fe}(\text{CN})_6] \cdot 4\text{H}_2\text{O}$ (II), and $[\text{Dy}_2(\text{Terpy})_2(\text{H}_2\text{O})_4(\text{CO}_3)(\text{NCS})\text{Fe}(\text{CN})_6] \cdot 11.4\text{H}_2\text{O}$ (III), which were structurally characterized.

EXPERIMENTAL

The following reagents were used: $\text{Dy}(\text{NCS})_3 \cdot 6\text{H}_2\text{O}$ [9], $\text{DyCl}_3 \cdot 6\text{H}_2\text{O}$, Terpy, and $\text{K}_3\text{Fe}(\text{CN})_6$ (all purchased from Aldrich). All procedures were carried out in air.

Synthesis of complex I. A weighed sample of $\text{Dy}(\text{NCS})_3 \cdot 6\text{H}_2\text{O}$ (0.045 g, 0.100 mol) was dissolved in H_2O (2.5 mL), and Terpy (0.0225 g, 0.096 mmol) was dissolved in EtOH (2 mL). A solution of Terpy was introduced into a solution of dysprosium thiocyanate

on stirring. The obtained homogeneous solution was carefully layered onto a solution of the cyanide salt $K_3Fe(CN)_6$ (0.034 g, 0.104 mmol) dissolved in H_2O (2.5 mL) with the addition of EtOH (2 mL). Orange crystals were immediately formed in the yellow-green solution. In a week, the orange solid phase was separated from the solution, washed with an ethanol–water (1 : 1) mixture, and dried in air. The yield of compound **I** was 0.060 g (80% based on Dy). The X-ray diffraction analysis showed the single-phase character of compound **I**.

A single crystal of $[Dy(Terpy)(H_2O)_3Fe(CN)_6] \cdot 4.8H_2O$ (**Ia**) was sampled from the solid phase of the product obtained from a $DyCl_3 \cdot 6H_2O$ –Terpy– $K_3Fe(CN)_6$ –MeOH– H_2O solution. Single crystals of compounds **II** and **III** were taken from the heterogeneous reaction mixture $Dy(NCS)_3$ –Terpy– $K_3Fe(CN)_6$ –EtOH– H_2O .

For $C_{21}H_{27}N_9O_8FeDy$ (**I**) ($FW = 751.84$)

Anal. calcd., %	C, 33.55	H, 3.62	N, 16.77
Found, %	C, 33.04	H, 3.52	N, 16.25

Elemental analysis was carried out according to standard procedures on an EA1108 Carlo Erba CHN analyzer at the Center for Collective Use of the Kurnakov Institute of General and Inorganic Chemistry (Russian Academy of Sciences). IR spectra with attenuated total reflection were recorded in a range of 400–4000 cm^{-1} on a Bruker ALPHA instrument.

X-ray diffraction analysis was conducted on a Bruker D8 Advance diffractometer (CuK_{α} , Ni filter, LYNXEYE detector) at the Center for Collective Use of the Kurnakov Institute of General and Inorganic Chemistry (Russian Academy of Sciences).

The static and dynamic magnetic susceptibilities of the complexes were measured on a Quantum Desing PPMS-9 magnetometer. The static magnetic susceptibility was measured in a range of 2–300 K in the magnetic field with an intensity of 5 kOe. The frequency dependences of the dynamic magnetic susceptibility were measured at 2 K and at various magnetic field intensities. To prevent the orientation of the crystals by the magnetic field, the samples were moistened with mineral oil, placed into plastic bags, and hermetically sealed. A correction to diamagnetism of the molecule was applied by the Pascal scheme, as well as corrections to the magnetism of the mineral oil and sample holder.

X-ray structure analyses of compounds Ia, II, and III. The experimental data were collected on a Bruker SMART APEX2 diffractometer (λMoK_{α} , graphite monochromator) [10] (Tables 1, 2). An absorption correction was applied semiempirically from the equivalents using the SADABS program [11]. The structures were determined by a combination of a direct method and Fourier syntheses. All the three

structures contain disordered solvate molecules of H_2O . In addition, one Terpy molecule and NCS are disordered in the structure of compound **II**. The populations of these fragments were obtained by the isotropic refinement of the structures with fixed thermal parameters of disordered atoms and were not refined in subsequent calculations. The hydrogen atoms of Terpy were calculated from geometric concepts and taken into account in the riding model. The positions of hydrogen atoms of water molecules were partially localized from the difference Fourier synthesis, partially calculated on the basis of hydrogen bond formation, and fixed in subsequent calculations. Positions of H atoms were not found for a series of disordered H_2O molecules. The structures were refined by the anisotropic–isotropic (some disordered atoms) least-squares method. All calculations were performed using the SHELXS-2016 and SHELXL-2016 program packages [12].

The experimental data for the structures of compounds **Ia**, **II**, and **III** were deposited with the Cambridge Crystallographic Data Centre (CIF files CCDC nos. 1827138–1827140; deposit@ccdc.cam.ac.uk or <http://www.ccdc.cam.ac.uk>).

RESULTS AND DISCUSSION

Compound **I** was isolated from DyX_3 –Terpy– $Fe(CN)_6$ – H_2O –ROH solutions with the molar ratio $Dy : Terpy : Fe = 1 : 1 : 1$. The yield of compound **I** was close to the quantitative one regardless of X (Cl, NCS) and ROH (R = Me, Et). In the chain structure of compound **Ia**, the Dy : Fe ratio is 1 : 1; the coordination sphere of Dy contains three oxygen atoms of three water molecules, three nitrogen atoms of one Terpy molecule, and two nitrogen atoms of two bridging cyanide groups; the coordination mode is DyN_5O_3 ; and the coordination number of Dy is 8. It should specially be mentioned that the coordination sphere of dysprosium contains no acidic ligands X, which are linked with the cation in the initial salt DyX_3 [9]. However, on prolong storage of heterogeneous solutions (without separation of the phase of **I**) in air at ambient temperature, CO_2 is absorbed from air and ensembles of **II** and **III** are formed. Interestingly, the coordination of one thiocyanate ion with Dy is retained in compounds **II** and **III** when the dimeric fragments of Dy with CO_3 are formed. These results are consistent with the data of the works where the uptake of atmospheric CO_2 by the reaction systems containing lanthanide complexes was observed for dysprosium acetate with the hydrazone ligand [13], the macrocyclic complexes of Ln (La, Nd, Sm, Eu, Gd, Tb, Lu, and Y [14], and the La complex with the polydentate N,O ligand [15].

The broad absorption bands at 3069, 3336, and 3554 cm^{-1} in the IR spectra of the samples of compound **I** are caused by the $\nu(H_2O)$ vibrations. The intense multicomponent band (corresponding to the

Table 1. Selected structural data and refinement results for compounds **I**–**III**

Parameter	Value		
Compound	Ia	II	III
<i>T</i> , K	150(2)	150(2)	150(2)
Crystal system	Monoclinic	Monoclinic	Triclinic
Space group	<i>P</i> 2 ₁	<i>P</i> 2 ₁ / <i>n</i>	<i>P</i> 1̄
<i>a</i> , Å	8.4562(4)	10.6823(11)	10.6681(6)
<i>b</i> , Å	18.9461(8)	14.0714(15)	12.7903(7)
<i>c</i> , Å	9.4249(4)	30.370(3)	20.6419(13)
α, deg	90	90	73.132(2)
β, deg	104.5660(10)	99.898(2)	82.732(2)
γ, deg	90	90	84.743(2)
<i>V</i> , Å ³	1461.45(11)	4497.1(8)	2669.2(3)
<i>Z</i>	2	4	2
ρ _{calcd} , g/cm ³	1.684	1.843	1.741
μ, mm ⁻¹	3.088	3.723	3.158
<i>F</i> (000)	732	2436	1386
Crystal size, mm	0.2 × 0.12 × 0.1	0.04 × 0.02 × 0.02	0.26 × 0.08 × 0.06
Range of θ, deg	2.233–30.634	2.159–27.102	2.091–30.549
Range of indices	–12 ≤ <i>h</i> ≤ 12, –27 ≤ <i>k</i> ≤ 27, –13 ≤ <i>l</i> ≤ 13	–13 ≤ <i>h</i> ≤ 13, –18 ≤ <i>k</i> ≤ 17, –38 ≤ <i>l</i> ≤ 38	–15 ≤ <i>h</i> ≤ 13, –18 ≤ <i>k</i> ≤ 18, –29 ≤ <i>l</i> ≤ 29
Collected reflections	20776	41931	30992
Independent reflections (<i>R</i> _{int})	8937 (0.0403)	9896 (0.0261)	15703 (0.0509)
Completeness to θ = 25.242°, %	100.0	99.7	99.9
Max, min transmission	0.7461, 0.5691	0.0999, 0.0601	0.7461, 0.6191
Constraints/parameters	1/364	216/754	6/662
GOOF	0.966	1.307	0.987
<i>R</i> ₁ , <i>wR</i> ₂ (<i>I</i> > 2σ(<i>I</i>))	0.0336, 0.0738	0.0446, 0.0922	0.0461, 0.0831
<i>R</i> ₁ , <i>wR</i> ₂ (whole array)	0.0384, 0.0758	0.0504, 0.0946	0.0905, 0.0960
Flack parameter	–0.006(7)		
Δ _{max} , Δ _{min} , e/Å ³	1.654, –1.605	2.209, –2.103	1.214, –1.474

v(CN) vibrations), which is centered at 2121 cm^{–1} (2116 cm^{–1} in the initial salt K₃[Fe(CN)₆]), is also observed. The presence of more than one such a band corresponds to different coordination modes of the CN ligands: terminal and bridging. Strong bands at 1599 and 1572 cm^{–1} corresponding to the v(CN) vibrations (1580 and 1558 cm^{–1} in the initial ligand) and absorption bands in a range of 1481–1434 cm^{–1} (1467–1419 cm^{–1} in free Terpy) caused by the v(CC) vibrations are detected for the Terpy ligand. The shift of these bands indicates the coordination of Terpy in compound **I**. The data on the IR spectra of compound **I** are consistent with the X-ray structure analysis results.

According to the X-ray diffraction analysis data, the structure of complex **Ia** is similar to that of [Dy(Terpy)(H₂O)₃Co(CN)₆] · 5H₂O [16]. The structures of compounds **I**–**III** are formed by polymer chains (Fig. 1) and solvate H₂O molecules. In compound **Ia**, the Dy : Fe ratio is 1 : 1, the bridging CN ligands in the environment of the Fe atom are in the *cis* position toward each other, and the N(6)Dy(1)N(5A) angle is 101° (bridging ligands). In compounds **II** and **III**, the Dy : Fe ratio is 2 : 1, the empirical formula of the independent unit of the polymer chain in compounds **II** and **III** differs by one H₂O molecule only, and the structure of the Dy₂(Terpy)₂(CO₃) fragment is similar. However, the binding of these fragments in the

Table 2. Lengths of Ln–O bonds (Å) in the structures of compounds **I**–**III**

Bond	d, Å		
	Ia	II	III
Dy(1)–O(1)	2.401(4)	2.365(4)	2.341(3)
Dy(1)–O(2)	2.313(4)	2.410(4)	2.338(3)
Dy(1)–O(3)	2.356(5)		
Dy(1)–O(4)		2.322(4)	2.332(3)
Dy(1)–O(5)			2.360(3)
Dy(1)–N(1)	2.476(4)	2.496(6)	2.482(4)
Dy(1)–N(2)	2.500(5)	2.506(5)	2.483(4)
Dy(1)–N(3)	2.528(5)	2.544(5)	2.481(4)
Dy(1)–N(5) (<i>x</i> + 1, <i>y</i> , <i>z</i>)	2.438(5)		
Dy(1)–N(6)	2.450(5)		
Dy(1)–N(7)		2.436(6)	2.436(4)
Dy(1)–N(8) (<i>–x</i> + 3/2, <i>y</i> + 1/2, <i>–z</i> + 1/2)		2.431(5)	
Dy(2)–O(1)			2.406(3)
Dy(2)–O(3)			2.444(3)
Dy(2)–O(6)			2.413(4)
Dy(2)–O(7)			2.423(4)
Dy(2)–N(4)			2.549(5)
Dy(2)–N(5)			2.553(4)
Dy(2)–N(6)			2.524(4)
Dy(2)–N(10)			2.468(4)
Dy(2)–N(13)			2.469(5)

structures of compounds **II** and **III** by the $\text{Fe}(\text{CN})_6$ complexes differs (Figs. 1b, 1c).

In the structure of compound **II**, the Dy(1) atom participates in the formation of the $\text{Fe}–\text{CN}–\text{Dy}–\text{NC}$ chain and the terminal Dy(2) atom adds to the chain via the CO_3^{2-} ligand. The bridging CN groups of complexes $\text{Fe}(\text{CN})_6$ are in the *cis* position toward each other, and the $\text{N}(7)\text{Dy}(1)\text{N}(8A)$ angle (bridging ligands) is 102° . If the Dy(2) atoms are conventionally rejected, then the structures of the chains in compounds **Ia** and **II** would be topologically similar. However, there is a distinction in the arrangement of the Dy and Fe atoms: in the structure of compound **Ia**, the Fe atoms are arranged at one side from the line connecting the Dy atoms, whereas they are arranged at different sides in the structure of compound **II**.

Both Dy atoms (as well as ligand CO_3^{2-}) are bridging in the polymer chain of the structure of compound **III**. Two crystallographically independent Fe atoms are localized in the inversion centers, which determines the *trans* arrangement of the bridging CN ligands: the $\text{N}(7)\text{XN}(10)$ angle is 151° (X is the center of the Dy(1)–Dy(2) section, and N(7,10) are the bridging nitrogen atoms).

The structures of the $\text{Dy}_2(\mu-\eta^4\text{CO}_3)$ fragment are the same in compounds **II** and **III**. All the six atoms lie in one plane with an accuracy of 0.06 Å, and the Dy...Dy distance is 4.74 Å. The mutual arrangement of Terpy in these structures differs: the screened arrangement in the structure of compound **II**, whereas in the structure of compound **III** the Terpy molecules are unfolded relative to each other (Fig. 2). Stacking interactions are observed between Terpy: the angle between the Terpy planes is 5° and 2° , and the shortest C...C distances are 3.26 and 3.40 Å in the structures of compounds **II** and **III**, respectively. The possibility of these interactions to occur is caused by the shift of the Dy atoms from the mean planes of Terpy by 0.16 and 0.68 Å (Dy(1) and Dy(2) in **II**) and 0.82 and 0.14 Å (Dy(1) and Dy(2) in **III**), respectively. The coordination number of Dy in the structures of compounds **I** and **II** is 8, whereas in compound **III** the coordination numbers of Dy(1) and Dy(2) are 8 and 9, respectively.

The study of the magnetic properties of compound **I** showed that $\chi T = 14.57 \text{ cm}^3 \text{ K/mol}$ at 300 K corresponds to a theoretical value of $14.54 \text{ cm}^3 \text{ K/mol}$ for the noninteracting Fe^{3+} iron ion in the low-spin state ($C = 0.37 \text{ cm}^3 \text{ K/mol}$) and the Dy^{3+} dysprosium ion: $^6H_{15/2}$, $C = 14.17 \text{ cm}^3 \text{ K/mol}$. The temperature depen-

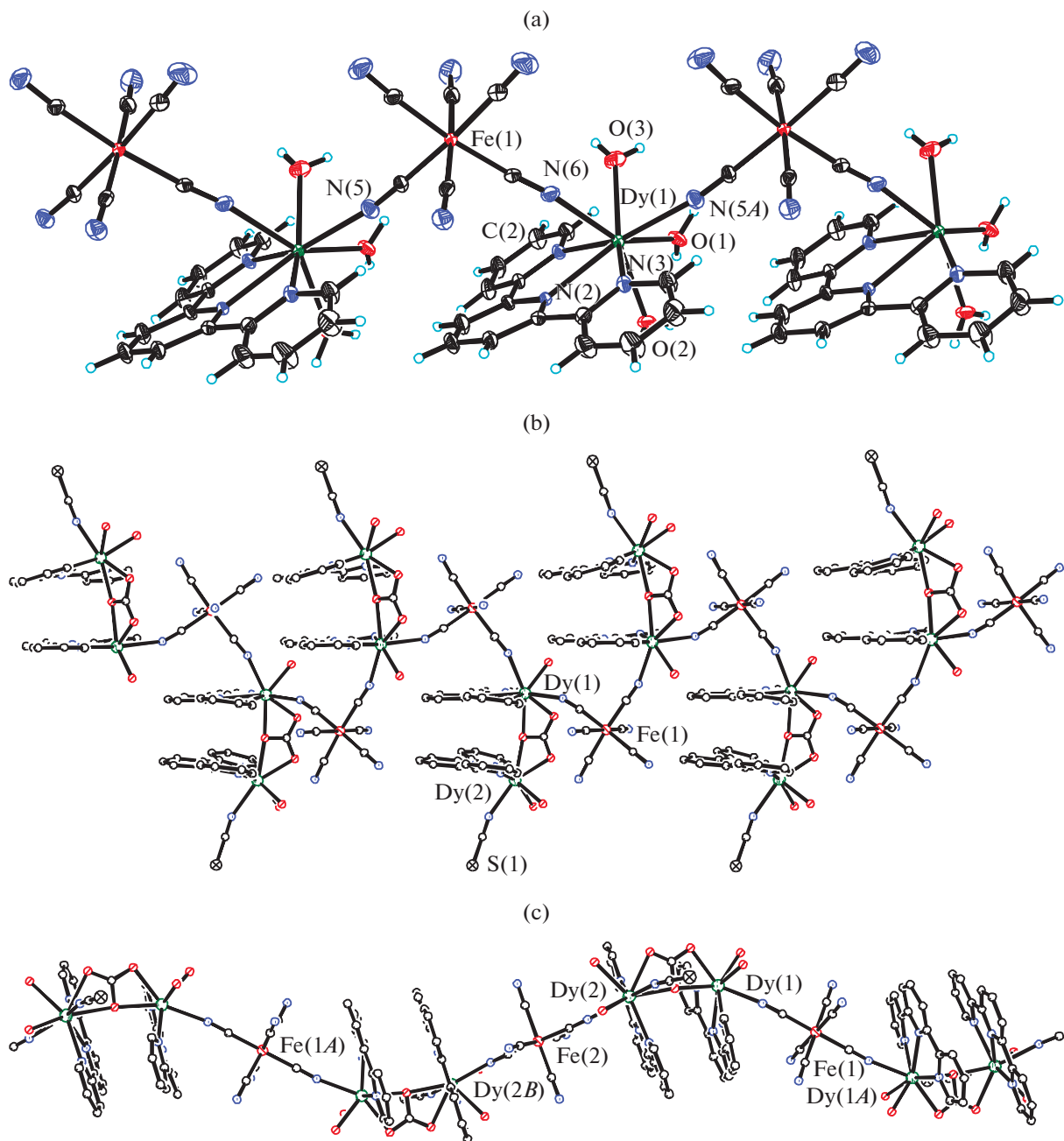


Fig. 1. Structures of the polymer chains in compounds (a) Ia, (b) II, and (c) III.

dence χT is presented in Fig. 3. It is seen that χT is almost temperature-independent down to $T = 100$ K. As the temperature decreases, χT begins to decrease, and further (below 12 K) a sharp decrease in the values of χT is observed. This behavior can be attributed to weak antiferromagnetic interactions in the chain between low-spin Fe^{3+} and Dy^{3+} and/or to a decrease in the population m_J of the levels of the Dy^{3+} ion split by the crystalline field, and also to the Zeeman effect in the applied magnetic field.

The dynamic magnetic susceptibility of compound I was measured at $T = 2$ K to establish the properties of the molecular magnetic. There are no values of the imaginary component χ'' of the dynamic magnetic susceptibility that differ from zero in the zero magnetic field in the whole frequency range (Fig. 4). The application of an external magnetic field decreases the probability of quantum tunneling of magnetization, which can lead to an increase in the relaxation time of the magnetization of the molecule. The measurements in external magnetic fields of vari-

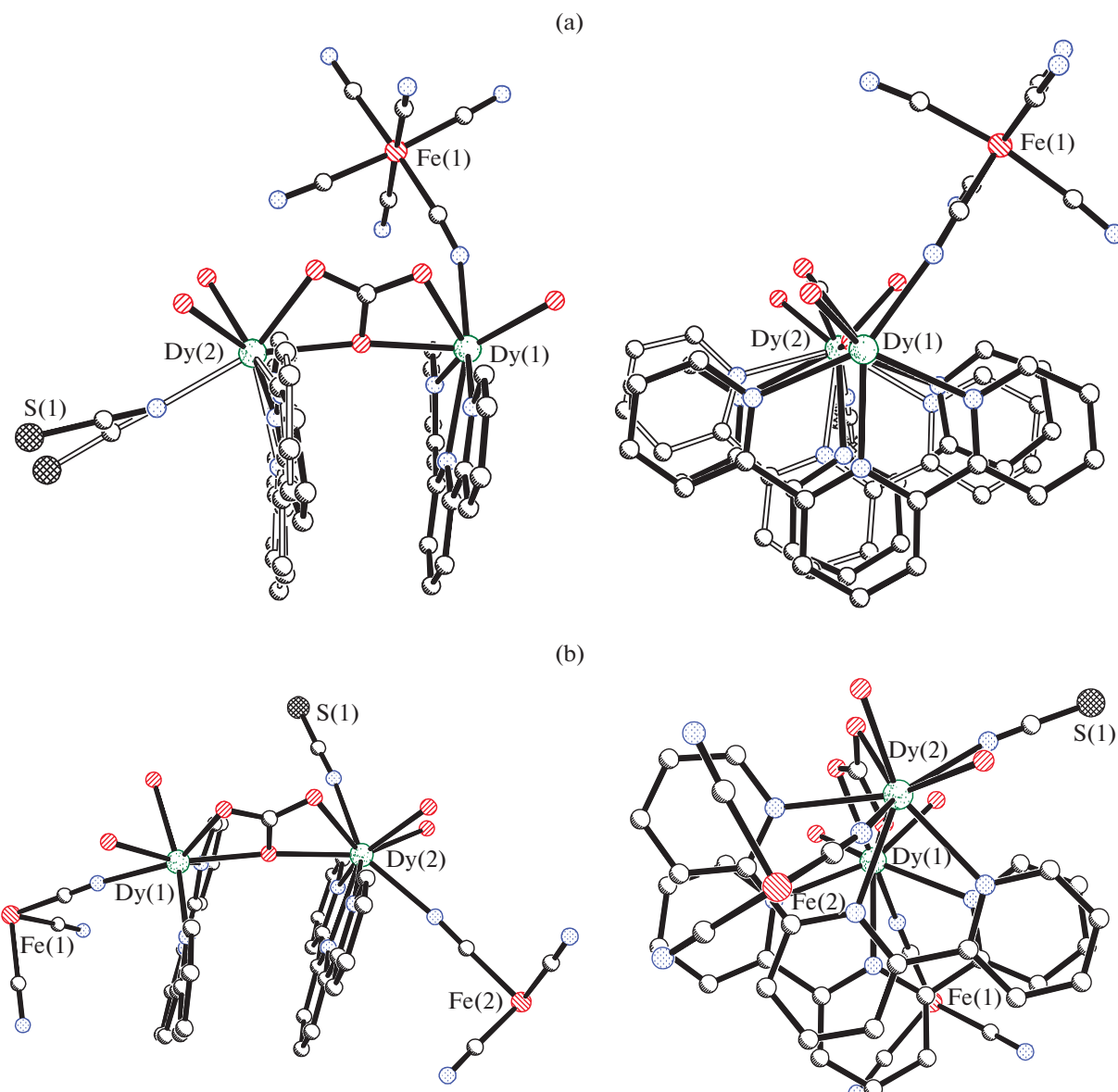


Fig. 2. Structures of the crystallographically independent fragments of the polymer chain for compounds (a) **II** and (b) **III**.

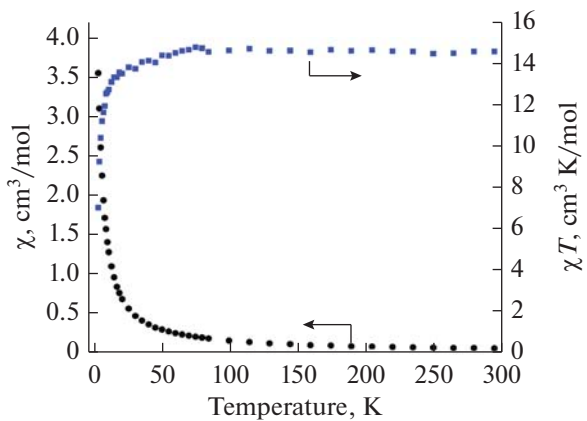


Fig. 3. Temperature dependences of the static magnetic susceptibility (●) χ and (■) χT for complex **I** in a magnetic field of 5 Oe.

ous intensities (0.5–1.5 kOe) found a noticeable deviation of χ'' from zero values. The imaginary part of the dynamic magnetic susceptibility increases with an increase in the frequency in a magnetic field of 0.5 kOe. In the fields with an intensity of 1 and 1.5 kOe, the absolute values χ'' almost twofold exceed similar values for the case of $H = 0.5$ kOe. However, no maxima are observed on the $\chi''(\nu)$ dependences in the accessible frequency range. This does not allow one to characterize the dynamics of the magnetic behavior of the substance, i.e., to determine the relaxation times and heights of the effective energy barrier for the magnetic reversal of the molecule. It should be mentioned that the fact that the detected values of the imaginary component of the dynamic magnetic sus-

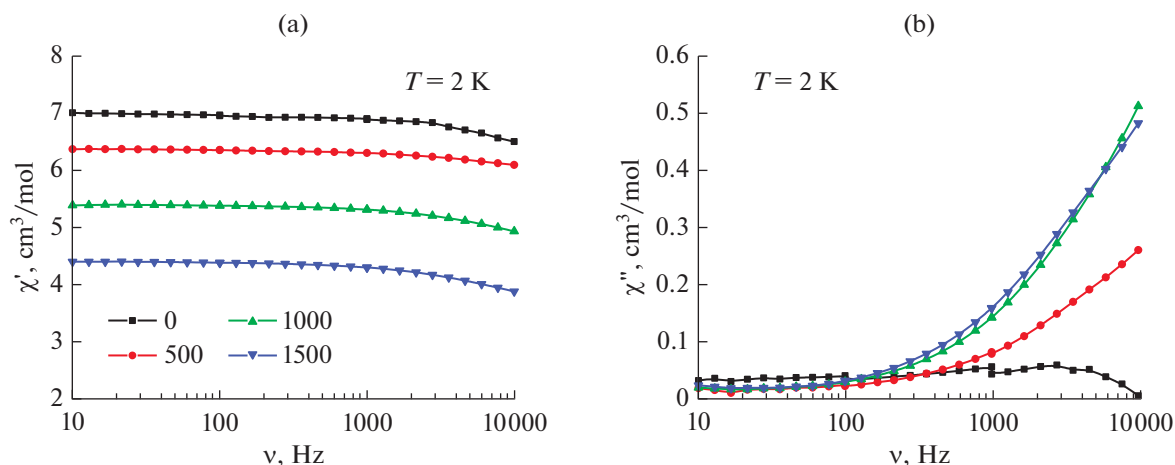


Fig. 4. Dependences of the (a) real (χ') and (b) imaginary (χ'') components of the dynamic magnetic susceptibility on the frequency for complex I in the external field of various intensities (0–1.5 kOe) at 2 K.

ceptibility differ from zero unambiguously indicates a slow magnetic relaxation in complex I.

ACKNOWLEDGMENTS

The authors are grateful for A.V. Gavrikov for recording IR spectra.

This work was supported by the Russian Science Foundation, project no. 14-13-00938.

REFERENCES

- Černák, J., Orendáč, M., Potočník, I., et al., *Coord. Chem. Rev.*, 2002, vol. 224, p. 51.
- Tanase, S. and Reedijk, J., *Coord. Chem. Rev.*, 2006, vol. 250, p. 2501.
- Pedersen, K.S., Bendix, J., and Clérac, R., *Chem. Commun.*, 2014, vol. 50, p. 4396.
- Dhers, S., Feltham, H.L.C., and Brooker, S., *Coord. Chem. Rev.*, 2015, vol. 296, p. 24.
- Petrosyants, S.P., *Russ. J. Inorg. Chem.*, 2013, vol. 58, no. 13, p. 1605.
- Figuerola, A., Diaz, C., Ribas, J., et al., *Inorg. Chem.*, 2003, vol. 42, p. 5274.
- Figuerola, A., Ribas, J., Casanova, D., et al., *Inorg. Chem.*, 2005, vol. 44, p. 6949.
- Zhao, H., Lopez, N., Prosvirin, A., et al., *Dalton Trans.*, 2007, no. 8, p. 878.
- Petrosyants, S., Dobrokhotova, Z., and Ilyukhin, A., *Eur. J. Inorg. Chem.*, 2017, p. 3561.
- APEx2 and SAINT*, Madison: Bruker AXS Inc., 2007.
- Sheldrick, G.M., *SADABS*. Göttingen: Univ. of Göttingen, 1997.
- Sheldrick, G., *Acta Crystallogr., Sect. C: Struct. Chem.*, 2015, vol. 71, p. 3.
- Tian, H., Wang, M., Zhao, L., et al., *Chem.-Eur. J.*, 2012, vol. 18, p. 442.
- Bag, P., Dutta, S., Biswas, P.P., et al., *Dalton Trans.*, 2012, vol. 41, p. 3414.
- Hołyńska, M., Clérac, R., and Rouzières, M., *Chem.-Eur. J.*, 2015, vol. 21, p. 13321.
- Petrosyants, S., Ilyukhin, A., Efimov, N., et al., *Inorg. Chim. Acta*, 2018, vol. 482, p. 813.

Translated by E. Yablonskaya